EPJ Web of Conferences **282**, 01010 (2023) https://doi.org/10.1051/epjconf/202328201010
SSP 2022

Precision measurements in the beta decay of ^{6}He

Mohamad Kanafani[1,*], *Xavier* Fléchard[1], *Oscar* Naviliat-Cuncic[1,2], *Gyang Davou* Chung[1], *Sylvain* Leblond[3], *Etienne* Liénard[1], *Xavier* Mougeot[3], *Gilles* Quéméner[1], *Adriana* Simancas Di Filippo[1,4], and *Jean-Charles* Thomas[5]

[1]Université de Caen Normandie, ENSICAEN, CNRS/IN2P3, LPC Caen UMR6534, F-14000 Caen, France
[2]Facility for Rare Isotope Beams and Department of Physics and Astronomy, Michigan State University, East Lansing 48824 MI, USA
[3]Université Paris-Saclay, CEA, List, Laboratoire National Henri Becquerel (LNE-LNHB), F-91120 Palaiseau, France
[4]Deutsches Elektronen-Synchrotron DESY, Notkestraße 85, 22607 Hamburg, Germany
[5]GANIL, CEA/DRF-CNRS/IN2P3, Bd Henri Becquerel, 14076 Caen, France

Abstract. We report here about the ongoing data analysis of an experiment performed at GANIL with a 25 keV $^{6}He^{+}$ beam to determine the Fierz interference term from the β particles energy spectrum.

1 Introduction

The ^{6}He beta decay played a fundamental role in establishing the V-A character of the weak interaction [1, 2]. The fact that ^{6}He decays into ^{6}Li by a pure Gamow-Teller transition made it attractive for searches of physics beyond the standard model. The Fierz interference term is one of the coefficients that can be used to probe new physics, since it is linearly dependent on exotic tensor and scalar couplings. The Fierz term can be accessed experimentally by high precision measurements of the shape of the β-energy spectrum.

2 Experimental setup

The apparatus is described in details in Ref [3]. An experiment with a low-energy beam of $^{6}He^{+}$ ions was performed at the Grand Accélérateur National d'Ions Lourds (GANIL), Caen. The $^{6}He^{+}$ ions were guided at 25 keV towards the surface of a fixed detector "det 1". A second identical and movable detector "det 2" is used to enclose the ions implantation region and to achieve a 4π solid angle as shown in Fig 1. The motion of "det 2" is accurately synchronized with the beam implantation and the data acquisition. The period of the cycles is chosen such as to determine with a sufficient precision the surrounding background. The detector coverage ensures the full collection of all β particles emitted by the implanted $^{6}He^{+}$ ions, eliminating thus any energy loss due to backscattering.

The detectors "det 1" and "det 2" are formed each of a cylindrical $YAlO_3$ Ce-doped inorganic scintillator (YAP) surrounded by an EJ-204 plastic scintillator. The two scintillators are mounted in a phoswich configuration in which both of them are read out by one single

*Corresponding author: kanafani@lpccaen.in2p3.fr

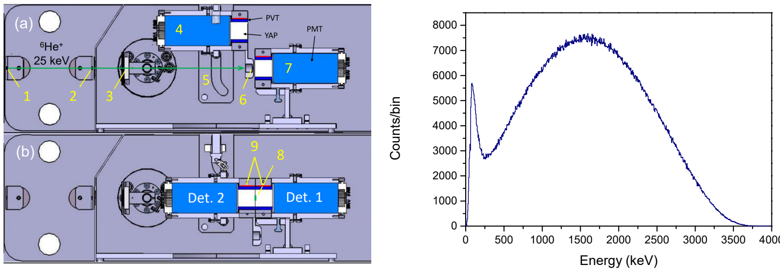

Figure 1. Left panel: sectional view of the experimental setup during beam implantation (a) and data taking (b). The labels on panel (a) are: 1 and 2– the two Ø6 mm collimators in the first section of the chamber; 3– a movable Si detector; 4 and 5– the moving detector and its mechanical guide; 6– the third Ø4 mm collimator; 7– the fixed detector. The green arrow indicates the ^{6}He^{+} beam. On panel (b), label 8 indicates the implantation region and 9 the two ^{241}Am calibration sources [3]. Right panel: experimental β-energy spectrum for one run of two hours duration.

photomultiplier tube (Fig 1). A 5-kBq ^{241}Am source is mounted on each of the detectors as illustrated in Fig 1. The 59.54 keV γ rays from the ^{241}Am were used as a reference to monitor gain and baseline variations during the experiment.

Each event is labeled with a time stamp and an energy charge integration, allowing a control over systematic effects in the offline analysis. Five sets of runs were taken with different experimental conditions, to study systematic and background effects [3].

3 Background investigation

The experimental β-energy spectra showed the expected continuous spectrum extending up to 3.5 MeV, the endpoint energy of ^{6}He decay, alongside with an unexpected contribution peaked at 0.1 MeV (Fig 1). This peak was also present in the background runs, where the ^{6}He beam was implanted on the collimator fixed to the moving detector, and not on the YAP (Fig 2). This peak was identified to be caused by β particles from the ^{6}He^{+} ions, interacting with the material of the collimator itself and generating Bremsstrahlung photons that are detected by the two detectors.

The experimental geometry with the two detectors and the collimator attached to "det 2" was built in GEANT4 (Fig 2), to validate the origin of this peak at low energy. Events were generated using the phase space of the ^{6}He decay, on the inner surface of the collimator as shown in Fig 2. The deposited energy spectrum inside the two YAP scintillators obtained by simulation was found to match the experimental spectrum up to 1 MeV (Fig 2, left).

A wide peak between 1.5 and 3 MeV, which is not reproduced by the former simulation, was also observed in the background data (Fig 2, left). This peak was attributed to electrons from ^{6}He decay, going through a hole in the lower part of the detector, which leads to the YAP scintillator of the movable detector through the plastic scintillator. Another simulation was then performed where the source of electrons was set on the outer surface of the collimator. The simulated spectrum of the deposited energy inside the YAP scintillators showed the appearance of the same distribution along with the Bremsstrahlung peak (Fig 2, center), confirming thereby the origin of these events.

For the β spectrum shape analysis, the presence of these two intruders within the β-energy spectrum will be suppressed by using data taken during the background runs.

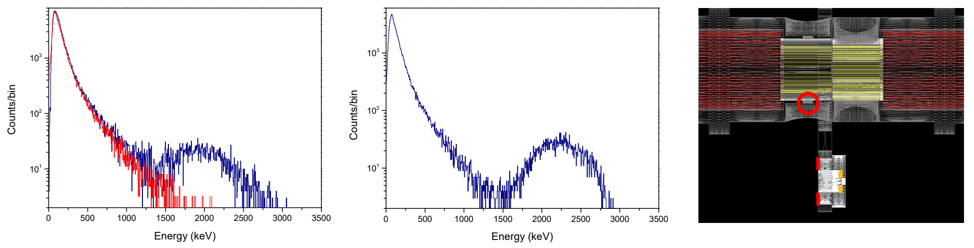

Figure 2. Left panel: the blue histogram is the experimental energy spectrum for one run where the ^{6}He was implanted on the collimator. The red histogram is the deposited energy spectrum obtained with simulation, normalized to the experimental data. Center panel: the deposited energy spectrum obtained with a simulation where the source of electrons is placed on the outer surface of the collimator. Right panel: the two detectors with the collimator built in GEANT4. The orange and red lines represent respectively the position of the source of events on the inner and outer surface of the collimator. The red circle shows the position of the hole through which the electrons of the decay on the collimator were able to access the YAP scintillator.

4 β-energy spectrum fit function

The energy distribution of the β particles emitted from ^{6}He decay can be written as:

$$N(W) \propto pW(W - W_0)^2 \left(\alpha_0 + \alpha_{-1} \cdot \frac{1}{W} + \alpha_1 \cdot W + \alpha_2 \cdot W^2\right) \tag{1}$$

where p, W and W_0 are respectively the momentum, total energy and the endpoint energy of the emitted electrons in unit of the electron mass. α_{-1}, α_0, α_1 and α_2 are coefficients that represent all the relevant corrections to the shape of the spectrum (the Fierz term is included in α_{-1}). It can be useful to have these coefficients fixed with different values or set as free parameters in the fitting procedure. However, this function cannot be used directly to fit the experimental β-energy spectrum, since it does not account for the energy loss due to Bremsstrahlung energy escape. In the following, we introduce a method used to account for Bremsstrahlung escape within an analytical model.

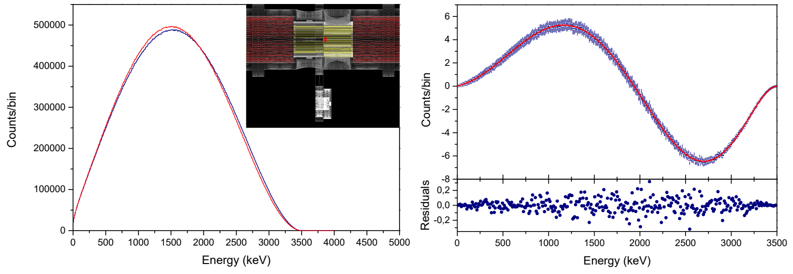

Figure 3. Left panel: the generated energy spectrum with Eq. (2) (in blue), and the deposited energy within the two YAP scintillators obtained by GEANT4 simulation (in red). Insert: the simulation geometry with the source of events placed between the two YAP scintillators (the red spot). Right panel: on top, the histogram of the normalized difference between the generated and deposited energy histograms (in blue). The fit of this histogram with a polynomial function (in red). On bottom, the residuals of the fit.

As a first step, four distributions of events were generated following the functions:

$$g_i(W) = pW(W - W_0)^2 \cdot W^i \tag{2}$$

where $i = -1, 0, 1, 2$. For each $g_i(W)$ distribution, the effect of the Bremsstrahlung escape was estimated using GEANT4. The energy spectra of the generated and the deposited energies were built for each of the four sets. The histograms of the normalized difference between the generated and deposited energy spectra were then plotted and fitted with a polynomial function $f_i(W)$ (Fig 3). These functions represent the effect of the Bremsstrahlung escape on each term of the energy spectrum.

The deposited energy spectrum resulting from the decay function of Eq. (1) and accounting for Bremsstrahlung escape can be expressed or fitted with:

$$F(W) = \alpha \sum_{i=-1}^{2} \alpha_i \left[g_i(W) + f_i(W)\right] \tag{3}$$

where α is a normalization factor and $f_i(W)$ are the polynomial functions that describe the effect of Bremsstrahlung energy escape for each term of the β-energy spectrum. These functions were tested with several statistically independent data sets generated in GEANT4 with Eq. (1) for several values of α_{-1}, α_0, α_1 and α_2. The deposited energy spectra were built afterwards and fitted with Eq. (3), where α_0, α_1 and α_2 were fixed parameters, while α and α_{-1} were free parameters.

The results of the fits were all statistically consistent with the values of α_1 that were initially used to generate the spectra. The standard residuals of the fit function, which are distributed around zero within $\pm 2\sigma$, also proved the validity of the fit function (Fig 3).

5 Summary

To summarize, the analysis of the spectrum shape of ^{6}He has been briefly introduced. Two background components present within the experimental β spectrum have been identified. They will be dealt with using background runs, during which $^6He^+$ ions were blocked from reaching the detector surface. The effect of the Bremsstrahlung energy escape on the shape of the β-energy spectrum was presented alongside how we plan to account for this effect with the addition of a polynomial analytical function which will be used later on to fit the experimental data.

This project was supported in part by the French Agence Nationale de la Recherche under grant ANR-20-CE31-0007-01 (bSTILED).

References

[1] C. H. Johnson, F. Pleasonton, and T. A. Carlson, Phys. Rev. **132**, 1149 (1963).
[2] J. B. Vise and B. M. Rustad, Phys. Rev. **132**, 2573 (1963).
[3] M. Kanafani, X. Fléchard, O. Naviliat-Cuncic, G. D. Chung, S. Leblond, E. Liénard, X. Mougeot, G. Quéméner, A. Simancas Di Filippo, and J.-C. Thomas, Phys. Rev. C **106**, 045502 (2022).